

Research article

Crystallization of e-beam evaporated amorphous InSe thin films after heat-treatment

J. Hossain^{*}, M. Julkarnain, K. S. Sharif and K. A. Khan

Department of Applied Physics & Electronic Engineering, University of Rajshahi, Rajshahi-6205, Bangladesh.

*E-mail: jak_apee@ru.ac.bd

Abstract

Indium selenide (InSe) thin films have been prepared by e-beam evaporation technique onto glass substrate at a pressure of $\sim 8 \times 10^{-5}$ Pa. The deposition rate of the InSe thin films is about 8.30 nm s^{-1} . The thickness of the films ranges from 60 to 600 nm, respectively. The virgin films show a structural transformation event at temperatures ranging from 415 K to 455 K which has been investigated by XRD, SEM, EDAX studies. X-ray diffraction (XRD) study reveals that InSe thin films are amorphous before heat-treatment while they are polycrystalline after heat-treatment where phase-transition occurs. After heat-treatment the films are named as phase-transited films. Scanning Electron Microscopy (SEM) has been used to study the surface morphology of InSe thin films. Before heat-treatment grains are absent in the films and the surfaces are almost smooth and uniform. The film surfaces are rough and they are seen to exhibit a number of grains after phase-transition i.e. after heat-treatment. The elemental composition of the InSe thin films has been estimated by Energy Dispersive Analysis of X-ray (EDAX) method. The optical study of InSe thin films is carried out in the wavelength range $360 < \lambda < 1100 \text{ nm}$ at room temperature. **Copyright © IJRETR, all rights reserved.**

Keywords: InSe thin films, e-beam technique, XRD, SEM, EDAX

1. Introduction

Indium Selenide (InSe) belongs to III –VI compounds family being a layered semiconductor consisting of covalent bonded units (Se-In-In-Se) held together by Van der Waals forces and is one of the most suitable compound semiconductors for optoelectronic and photovoltaic applications [1]. Being a layer-type semiconductor, its two-dimensional structure and its resulting anisotropic properties are of particular interest. Literature reports indicate that InSe thin films have been prepared by a number of techniques by a number of researchers. These include the vacuum evaporation [2, 3, 4], flash evaporation [5], molecular beam deposition [6], electrodeposition [7], sol-gel method [8], etc.

In the present work, it has been observed that when the virgin samples are heated to a temperature ranges from 415 to 455 K, a phase transition phenomenon occurs i.e. the structure of the films changes. This structural transformation of the films has been investigated by XRD, SEM, electrical and optical studies.

2. Experimental

Indium selenide (InSe) thin films have been prepared by e-beam evaporation technique onto glass substrate at a pressure of $\sim 8 \times 10^{-5}$ Pa from InSe granular powder (99.999%) obtained from Materials by Metron, USA. Before deposition, the deposition chamber was thoroughly cleaned with emery paper and cotton wool by wetting acetone and was then dried with a dryer. A small quantity of source materials was loaded into clean cermet hearth based on the source turret. The glass substrates were then first cleaned in chromic acid solution and then washed in distilled water. After washing and drying in hot air, the substrates were then again cleaned in acetone and dried in hot air, and were then used for deposition. Finally, the cleaned substrates were placed on the substrate holder about 0.09 m above the source turret and the chamber bell-jar was placed on the base plate. A mechanical shutter was operated from outside, isolated the substrates from the evaporants. When the chamber pressure reduced to $\sim 8 \times 10^{-5}$ Pa, the deposition was then started with 30 mA current by turning on the low-tension control switch. All the films were deposited at room temperature. The film thickness was measured by the Tolanasky interference method with an accuracy of ± 5 nm [9].

3. Results and Discussion

3.1 X-ray Diffraction (XRD) Study

The X-ray diffraction of InSe samples has been done using a diffractometer, PHILIPS model "X'Pert PRO XRD System". X-ray diffractograms of all the samples have been recorded using monochromatic $\text{Cu K}\alpha$ radiation ($\lambda = 1.54187 \text{ \AA}$), scanning speed 2 degree/min, starting from 8° and ending at 50° to ensure the information of the single phase nature of the sintered product. The peak intensities are recorded corresponding to their 2θ values. The XRD patterns of InSe sample of thickness 300 nm is shown in Figure 1. From these patterns it is seen that the virgin films are amorphous in nature. And phase-transited InSe films have remarkable peaks. So it can be concluded that amorphous InSe thin films become polycrystalline after structural transformation. The similar phenomena have been investigated by other researchers [3, 10, 11]

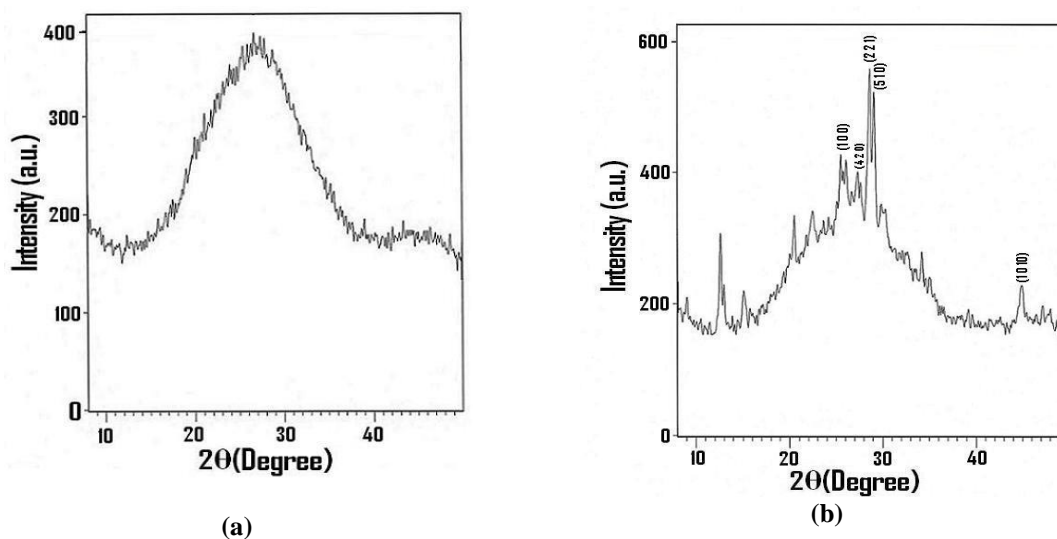


Figure 1: XRD spectra for (a) virgin and (b) heat-treated (phase-transited) InSe thin films of thickness 300 nm.

The d_{hkl} values are calculated from the intensity peaks of the XRD spectra for InSe thin films. These calculated values are compared with ASTM card's d_{hkl} values, and their corresponding planes and card's number, respectively are tabulated in Table 1. According to XRD results, the InSe thin films are polycrystalline hexagonal system with lattice parameters: $a = 19.20 \text{ \AA}$, $b = 19.20 \text{ \AA}$ and $c = 4.00 \text{ \AA}$, respectively.

Table 1: Comparison of d-values with ASTM data for phase-transited InSe thin films after heat-treatment

Thickness, t (nm)	2θ (Deg)	(Observed) d_{hkl} (Å)	ASTM Standard			
			2θ (Deg)	d_{hkl} (Å)	Planes (hkl)	Ref. code #
240	26.1286	3.41055	26.111	3.410	1 0 1	00-034-1431
	28.6562	3.11522	28.401	3.140	4 2 0	00-012-0118
	29.1451	3.06406	29.258	3.050	2 2 1	00-012-0118
300	25.7082	3.46537	25.689	3.465	1 0 0	00-034-1431
	28.6937	3.11124	28.401	3.140	4 2 0	00-012-0118
	29.1175	3.06691	29.258	3.050	2 2 1	00-012-0118
	30.148	2.96438	30.168	2.960	5 1 0	00-012-0118
	44.8288	2.02018	44.281	2.0439	1 0 10	00-029-0676

The crystallite size (D) of the films has been calculated from the Debye Scherrer's formula from the full-width at half-maximum (FWHM) β of the peaks expressed in radians [12]

$$D = \frac{0.94\lambda}{\beta \cos\theta} \quad (1)$$

where, λ is the wavelength of the X-ray used, β is the FWHM calculated for different planes.

The dislocation density (δ), defined as the length of dislocation lines per unit volume of the crystal, has been calculated by using the formula [13]

$$\delta = \frac{1}{D^2} \quad (2)$$

The strain (ϵ) is calculated from the slope of $\beta \cos\theta$ versus $\sin\theta$ plot using the relation [13]

$$\beta = \frac{\lambda}{D \cos\theta} - \epsilon \tan\theta \quad (3)$$

The crystallite size, dislocation density and strain have been calculated and are shown in Table 2

Table 2: Properties of e-beam evaporated phase-transited InSe thin films after heat-treatment

Film thickness, t (nm)	Planes (hkl)	Observed β (FWHM) (Rad) $\times 10^{-3}$	Crystallite size, D (nm)	Dislocation density, δ (lin/m^2) $\times 10^{14}$	Strain, ϵ ($\text{lin}^{-2} \cdot \text{m}^{-4}$) $\times 10^{-3}$
240	1 0 1	5.496	27.072	13.645	1.512
	4 2 0	1.889	79.176	1.595	0.472
	2 2 1	1.374	109.025	0.841	0.337
300	1 0 0	8.243	18.034	30.746	2.306
	4 2 0	1.717	87.109	1.318	0.429
	2 2 1	1.545	96.891	1.065	0.380
	5 1 0	5.496	27.311	13.407	1.303
	1 0 10	3.770	41.587	5.782	0.583

It is seen from Table 2 that the crystallite size varies from 18.034 to 109.025 nm, dislocation densities varies from 0.84×10^{14} to $30.746 \times 10^{14} \text{ lin}/\text{m}^2$ and strain varies from 0.337×10^{-3} to $2.306 \times 10^{-3} \text{ lin}^{-2} \cdot \text{m}^{-4}$ in the InSe samples. It is also seen that as the crystallite size of the film increases both the dislocation density and strain decreases.

3.2 Scanning Electron Microscopy (SEM) & EDAX Study

Figure 2 shows the SEM images of the InSe thin films of thickness 240 nm. These SEM images indicate that there is no sign of grains in the virgin films and the surfaces are almost smooth and uniform. While there are a number of grains in the phase-transited InSe thin films and the surfaces are rough. From these figures it is evident that InSe thin

films become polycrystalline after phase-transition due to heat-treatment which has also been verified by XRD study.

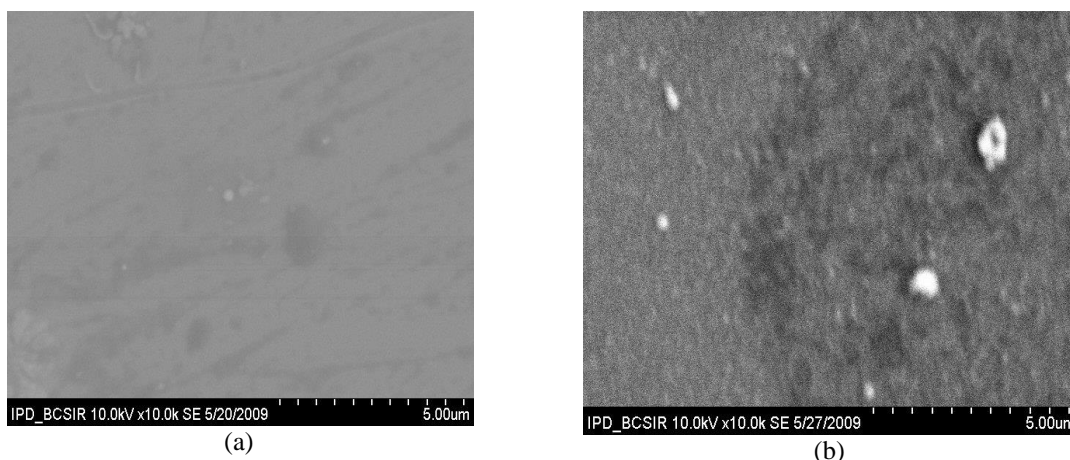


Figure 2: The SEM images of (a) virgin and (b) heat-treated (phase-transited) InSe thin films of thickness 240 nm.

The analysis of the elemental compositions for the InSe thin films of various thicknesses were estimated by using the method of Energy Dispersive Analysis of X-ray (EDAX). The result of elemental composition by EDAX study for InSe thin films of thickness 240 and 300 nm, respectively is shown in Table 3.

Table 3: Elemental composition of InSe thin films of variable thickness

Thickness (nm)	EDAX Results		Remarks
	In(%wt)	Se(%wt)	
240	70.68	29.32	Virgin
	70.75	29.25	Phase-transited
300	70.05	29.95	Virgin
	70.58	29.42	Phase-transited

3.3 Temperature Effect on Electrical Conductivity

Temperature dependence of electrical conductivity has been studied for the virgin InSe thin films. Electrical conductivity σ has been measured as a function of temperature T in the 305-475 K range. The glass substrate was heated by a specially designed heater and the temperature was measured by a chromel-alumel thermocouple placed on the middle of the substrate. The conductivity was obtained by applying a d.c.0-15 V bias across the films with silver contact and recording the current and voltage simultaneously by using a standard four-probe Van-der-Pauw technique [14].

Figure 3 shows the $\ln\sigma$ versus inverse absolute temperature curves for the four InSe thin films of different thicknesses prepared at room temperature. It is seen from the figure that the conductivity increases continuously with temperature and a sharp increase in conductivity is observed at a temperature which varies with thickness. This phase change of conductivity is irreversible, i.e. it does not return to the initial state. The irreversible temperature dependence of electrical conductivity reveals the changes in the film structure during heat treatment and improvement in the crystallinity of the film [3, 10, 11, 15].

The activation energies of the films have been calculated from the slopes of the curves. The activation energy and grain size of the InSe thin films are shown in Table 4.

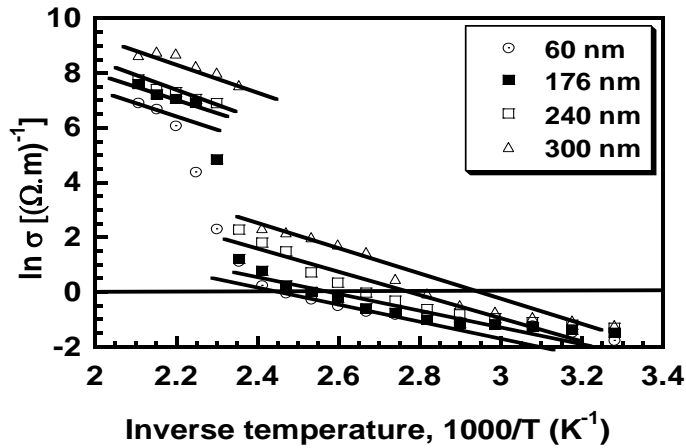


Figure 3: Variation of $\ln \sigma$ with inverse temperature for virgin InSe thin films.

Table 4: Activation energies and grain sizes evaluated for four InSe thin films.

Film thickness (nm)	Activation energy, ΔE (eV)	
	Before phase-transition	After phase-transition
60	0.675	0.786
176	0.697	0.652
240	0.690	0.708
300	0.686	0.566

3.4 Optical study

Spectral transmittance $T(\lambda)$ and near normal reflectance $R(\lambda)$ of InSe thin films have been measured at wavelength $0.36 < \lambda < 1.1 \mu\text{m}$ using SHIMADZU UV-Visible double beam spectrophotometer. The transmittance of virgin and phase-transited InSe thin films of thicknesses 176, 240 and 300 nm are shown in Figure 4(a) and 4(b), respectively.

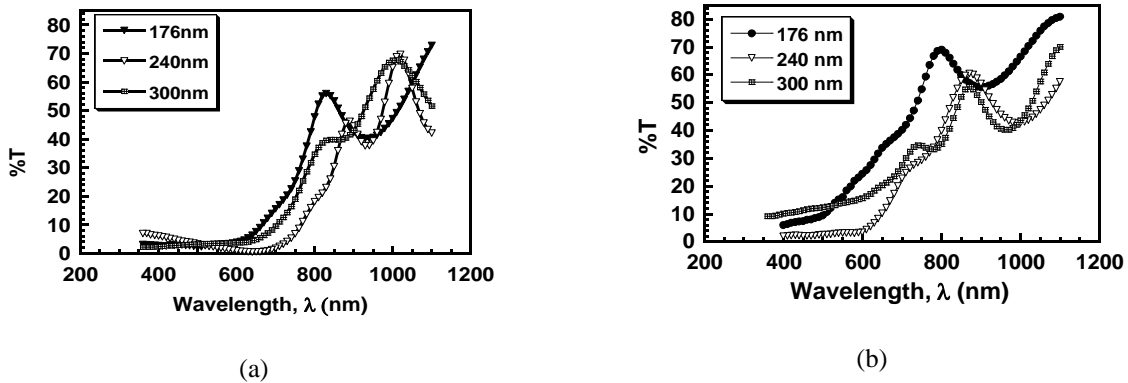


Figure 4: Variation of transmittance with wavelength of (a) virgin and (b) heat-treated (phase-transited) InSe films of different thicknesses.

In order to determine the value of optical band gap, $(\alpha h\nu)^{1/n}$ vs. photon energy ($h\nu$) curves have been plotted. The values of the tangents, evaluated by least mean square method, intercepting the energy axis give the values of optical band gap (E_g). From these curves it is observed that best fit is obtained for $(\alpha h\nu)^2$ vs. ($h\nu$) plot which indicates direct allowed transition. The variations of direct band gap with thickness are given in Table 5.

Table 5: Optical band gap of InSe thin films

Thickness, t (nm)	Virgin thin films	Phase-transited thin films due to heat-treatment
	Direct band gap (eV)	Direct band gap (eV)
176	1.65	1.92
240	1.64	1.76
300	1.60	1.68

The calculated values of direct band gap (E_g) for different thickness of virgin InSe samples vary between 1.60 to 1.65 eV which well agree with early reports [3, 16, 17]. It is shown from the table that band gap slightly decreases with thickness. This decrease of band gap with thickness may be attributed to the presence of unstructured defects, which increase the density of localized states in the band gap and consequently decrease the energy gap [18]. The calculated values of direct band gap (E_g) for different thickness of phase-transited InSe samples vary between 1.68 to 1.92 eV.

The observed change of band gap of the virgin and phase-transited films can be partially explained- on the basis of the model of the density of states in amorphous solids proposed by Mott and Davis [19]. According to this model, the width of the localized states near the mobility edges depends on the level of disorder and defects present in the amorphous structure. In particular, it is known that unsaturated bonds together with some saturated bonds are produced as a result of non-stoichiometry of the components in the amorphous films. The unsaturated bonds are responsible for the formation of some defects in the films. Such defects produce the localized states in the amorphous solids. The presence of a high concentration of localized states in the band structure is responsible for the low value of E_g in the case of room temperature deposited amorphous films. In the process of heated films (i.e. in polycrystalline films), the unsaturated defects are gradually annealed out producing a large number of saturated bonds. The reduction in the number of unsaturated defects decreases the density of localized states in the band structure, consequently increasing the optical band gap [20].

4. Conclusion

The XRD patterns reveal that after heat-treatment and phase-transformation the amorphous InSe thin films become polycrystalline. The SEM study shows that there is no sign of grains in the virgin films and the surfaces are almost smooth and uniform. While there are a number of grains in the heat-treated (phase-transited) InSe thin films and the surfaces are rough. The electrical study shows that when the temperature is raised to 415 to 455 K the conductivity of the InSe thin films increases abruptly indicating structural transformation of the films. The optical study exhibits that band gap of the films is increased after structural change due heat-treatment in the film as compared to the virgin film.

Acknowledgements

One of us, J. Hossain is indebted to Mrs. Nazia Sultana, SEM Operator, BCSIR, Dhaka, Bangladesh for her kind help during the study of SEM and EDAX.

References

- [1] Y. Hasegawa, Y. Abe, Phys. Stat. Sol. A79,615 (1982).
- [2] M. Peršin, B. Čelustka, B. Markovič and A. Peršin, Thin Solid Films 5, 123-128(1970).
- [3] C. Viswanathan, G. G. Rusu, S. Gopal, D.Mangalaraj, Sa. K. Narayandass, J. of Optoelectronics and Advanced Materials 7, 705-711 (2005).
- [4] M. Di Giulio, G. Micocci, R. Rella, P. Siciliano and A. Tepore, Thin Solid Films148, 273-278 (1987).
- [5] M. Peršin, A. Peršin, B. Čelustka, Thin Solid Films 12, 117-122 (1972).

- [6] J. Y. Emery, L. Brahim-Otsmane, M. Jouanne, C. Julien and M. Balkanski, *Materials Science and Engineering B* 3,13-17(1989).
- [7] S. Gopal, C. Viswanathan, B. Karunagara, Sa. K. Narayandass, D. Mangalaraj, and Junsin Yi, *J. of Cryst. Res. Technol.* **40**, 557-562 (2005).
- [8] I. H. Mutlu, M. Z. Zarbaliyev and F. Aslan, *J. of Sol-Gel Science and Technology* 43, 223-226 (2007).
- [9] S. Tolansky, *Multiple beam interferometry of surface and films*, Oxford University Press, London (1948).
- [10] S.N. Grigorov, V.M. Kosevich, S.M. Kosmachev, A.V. Taran, *Physics and Chemistry of Solid State* 5, 35-37 (2004).
- [11] G. G. Rusu, *J. of Optoelectronics and Advanced Materials* **3**, 861(2001).
- [12] B. D. Cullity, "Elements of X-Ray Diffraction", Addison-Wesley, Reading, MA, p.102 (1972).
- [13] G. B. Williamson and R. C. Smallman, *Philos. Mag.* 1, 34 (1956).
- [14] Van-der-Pauw. *Philips Res. Rept.*, 13, 1 (1958).
- [15] C. Julien, M. Eddrief, K. Kambas and M. Balkanski, *Thin Solid Films* 137,27-37 (1986).
- [16] C. Viswanathan, V. Senthilkumar, R. Sriranjini, D. Mangalaraj, Sa. K. Narayandass, Junsin Yi, *Crystal Research and Tech.*40, 658 – 664 (2004).
- [17] A.F. Qasrawi, *Optical Materials* 29,1751-1755 (2007).
- [18] H. El-Zahed, A. El-Korashy, and M. Abdel Rahman, *Vacuum* 68, 19 (2002).
- [19] N. F. Mott and E.A. Davis, *Electronic Process in non-crystalline materials*, 2nd Edn, Clarendon Press, Oxford (1979).
- [20] M. Parlak and Ç. Erçelebi, *Thin Solid Films* 322, 334-339 (1998).